

Reactive sintering of boron-doped $\text{Ni}_{76}\text{Al}_{24}$ intermetallic

S. O. MOUSSA, K. MORSI

Department of Mechanical and Aerospace Engineering, University of Missouri, Columbia, Missouri, MO 65211, USA

E-mail: morsik@missouri.edu

A preliminary investigation into the formation of boron-doped nickel-rich Ni_3Al with boron additions up to 2 wt% (i.e. to levels above the equilibrium solid solubility limit of boron in Ni_3Al) from elemental powders by reaction synthesis was carried out. The application of reaction synthesis was seen as a low-energy alternative to the production of Ni_3Al /boride composite suitable for wear applications. X-ray diffraction, Neutron diffraction, SEM/EDS, WDS, Image analysis, Archimedes principle and Rockwell hardness measurements; were used to study the effect of boron addition on the final microstructure, average grain size, bulk density and hardness of as-prepared $\text{Ni}_{76}\text{Al}_{24}$. Up to 0.3 wt% boron content, the microstructure consisted of single-phase Ni_3Al , however, at a boron content of 0.5 wt% an apparent transition from a single phase microstructure to a two-phase intermetallic/boride composite microstructure was observed, which dominated when the boron content increased, up to 2 wt%. The two-phase microstructure was identified as Ni_3Al (particles) within an $\text{Ni}_{41}\text{Al}_5\text{B}_{12}$ boride matrix, with no remaining un-reacted boron. The boron addition was found to increase the Rockwell hardness of Ni_3Al via two mechanisms. Below the solubility limit, the increase in hardness was due to solution hardening. Above 0.5 wt%B, solution hardening in addition to the formation of the harder boride phase, were found to amount to up to 50% increase in the hardness compared with boron free Ni_3Al . The extrusion of semi-molten beads at the surface of the compact at high B-content may be a limiting factor, in the formation of Ni_3Al /boride composites via this route. © 2002 Kluwer Academic Publishers

1. Introduction

The nickel aluminide intermetallic Ni_3Al is arguably considered the most promising nickel aluminide for industrialization in bulk form. The material exhibits outstanding properties including excellent corrosion, oxidation and carbonization/choking resistance [1]. It is well known that polycrystalline Ni_3Al is extremely brittle, exhibiting almost no ductility at ambient temperature. However, micro-alloying additions to the Ni_3Al compound can have significant improvements on the final properties of the intermetallic, thus enabling its use in a variety of structural applications [1–3]. The addition of small amounts of boron to the nickel-rich Ni_3Al intermetallic can lead to room temperature ductility enhancements of around 50% [4].

The yield strength of Ni_3Al was also reported to increase significantly as the boron content increased, reaching its peak values around the boron solubility limit in Ni_3Al . However, when the boron content exceeded its solubility limit and reached 0.470 wt%, the yield strength was found to decrease [5].

Previous work has shown that when the boron content exceeds its solubility limit in Ni_3Al , boron combines with nickel and aluminum atoms to form a boride phase with an f.c.c structure [4, 5]. In these studies

boron-doped nickel aluminides of both Ni_3Al and dual phase $\text{Ni}_3\text{Al} + \text{NiAl}$ compositions produced using a casting technique followed by heat treating and subsequent annealing were investigated [4, 5].

Casting is not the only route for the fabrication of Ni_3Al . Reaction synthesis, SHS (self propagating high temperature synthesis) has been extensively applied to the low-energy formation of these important alloys in binary form using a variety of configurations [6–9]. In its basic form it involves mixing elemental powders of e.g. nickel (Ni) and aluminium (Al) in the correct proportion to form the desired intermetallic compound e.g. Ni_3Al . The elemental powders are pressed into a green compact and heated to a temperature above the melting point of aluminium (typically 700°C), at which an exothermic reaction proceeds consuming the elemental powders and forming the intermetallic. The heat of reaction heats up the compact to significantly high temperatures for a short period of time. Although a great deal of work has been published on the reaction synthesis of binary nickel aluminide intermetallics, little work has been reported on the reaction synthesis of ternary Ni_3Al alloy compositions from elemental powders, especially in relation to boron additions [10]. It has been reported that the solubility limit of

boron in Ni₃Al is approximately 0.3 wt% [4]. In other work, using atom probe analysis the solubility limit reported was 0.2 wt% [5]. Only the reaction synthesis of 3Ni + Al (+0.10 wt%B) has been reported [6, 7] and no systematic study has been carried out in the fabrication of boron-doped nickel aluminide intermetallics via reactive sintering with the variation of boron content to a value above the reported solubility limit. It is of interest to examine the possibility of forming intermetallic/boride composite with possible improved wear resistance, in addition to examining how the rapid heating and cooling associated with reaction synthesis will affect the final microstructure. Will the boron dissolve in Ni₃Al to form solid solution or combine with nickel and aluminum atoms to form boride precipitates, or remain after the reaction and require homogenization as recently reported for reaction synthesis of chromium-doped iron aluminides [11]. Since the size of the boron atom (0.082 nm) is approximately three times smaller than that of chromium [12] it may aid faster diffusion rates during the reaction. It was also recently reported that boron diffuses 10³–10⁴ faster than nickel in Ni₃Al through octahedral interstitial sites [13]. This paper provides a preliminary investigation into the effect of alloying additions of boron to levels below and above the reported solubility limit in Ni₃Al on the reactive sintering of boron-doped Ni₇₆Al₂₄ alloy.

2. Experimental procedure

Nickel powder (99.99% pure, 6 μm in diameter) and gas-atomised aluminium powder (99.99% pure, 1–5 μm) were mixed in the molar proportion of 3 : 1 Nickel rich (76 at.% Ni), with the addition of zero, 0.05, 0.1, 0.3, 0.5, 1 and 2 wt% boron powders (99.8% pure, 6 μm). The powder mixtures were prepared in small batches and mixed for 30 min using a turbula mixer (GIENMILLS INC., 395 Allwood, Clifton, NJ 07012), the elemental powder mixtures were then compacted into a cylindrical pellet of initial density equal to 70 ± 2%. The cylindrical samples had diameter of 1.1 cm and height of 1.45 ± 0.1 cm. The compacts were then reaction synthesised by heating in a furnace under vacuum at a heating rate of 5°C/min. to a temperature of 700°C, and held for 15 minutes.

The bulk density of the intermetallic produced was measured using Archimedes principle. The specimens were then sectioned using an abrasive cutting wheel and mounted in conductive epoxy resin (copper filled) (BUEHLER LTD.). Grinding was carried out using 1200 SiC grit paper, followed by polishing using first 15 μm diamond finish, and finishing with 1–3 μm diamond finish.

In order to measure the average grain size and the effect of boron addition on the final microstructure, etching was carried out using a mixture of 20 vol% HCl + 20 vol% HNO₃ for 2–5 minutes. Using ASTM standard [14] and Image analysis (BUEHLER LTD.), the average grain sizes of the as prepared Ni₃Al & Ni₃Al-B-doped were measured.

Heat treatment was carried out using a Carbolite Tube Furnace (CARBOLITE LTD.).

Both XRD (Scintag PADV automated microprocessors control X-ray powder diffractometer) and Neutron Diffraction (2 XD Powder Diffractometer at the University of Missouri Research Center) were used to detect the phases present after reactive sintering. Also, SEM/EDS (Energy Dispersive Spectroscopy) and WDS (Wavelength Dispersive Spectroscopy) (AMRAY-600) were used to examine the distribution of Aluminium, Nickel, and boron in the microstructure obtained of as-etched nickel aluminides containing 1 wt% Boron.

3. Results and discussion

3.1. Effect of boron additions on the bulk structure, the final microstructure and the Rockwell hardness of as-prepared Ni₇₆Al₂₄ alloys

Initial examination of the compacts showed the appearance of semi-molten beads at the surfaces of the compact for samples with boron contents of 1 wt% and higher. The beads may have formed as a result of the presence of a higher volume liquid phase in the dual-phase product during the reaction.

Fig. 1 is an optical micrograph of as-etched nickel aluminides (boron-free and boron-doped) containing zero wt% Fig. 1a, 0.30 wt% Fig. 1b 0.50 wt% Fig. 1c and 1 wt% boron Fig. 1d. The data reveals that both boron-free and boron additions up to 0.30 wt%, alloys show a single-phase structure composed of equiaxed grains of boron-doped Ni₃Al. The average grain size appears to increase with the addition of boron up to 0.3 wt%; this is in contrary to recent work which shows boron to act as a grain growth inhibitor [15]. The previous work however did not involve reactive sintering, which may have a considerable effect as a non-equilibrium process on the final microstructure. Auger analysis may shed some light as to the amount of boron within the grain and at the grain boundaries of the single-phase, compared to reported values. This may certainly have an effect. No work to date has reported the effect of boron addition on grain size of reaction synthesized Ni₃Al.

However, when the boron content reached 0.5 wt% a clear transition from a single-phase microstructure to a two-phase one was observed. A two-phase microstructure dominated when the boron content increased to 2 wt%. SEM/EDS analysis (Ni/Al/B) of the two-phase microstructure was 85.1/14.8/0.1, and 90/5.5/4.5 wt% in the particle and the matrix respectively. According to this data, a two-phase microstructure was identified to consist of Ni₃Al (Al-rich) (particles) + Ni₄₁Al₅B₁₂(matrix), and indeed this finding was confirmed by both XRD and Neutron diffraction measurements. This two-phase microstructure was retained after heat treatment at 1000°C for 5 hours.

The two-phase microstructure obtained resembles a typical liquid phase sintered microstructure, with rounded particles in a matrix that is produced as a result of the matrix phase having a lower melting point than the particles. The matrix phase is therefore present as a molten liquid at the high temperatures achieved during the reaction. The formation of this liquid phase will

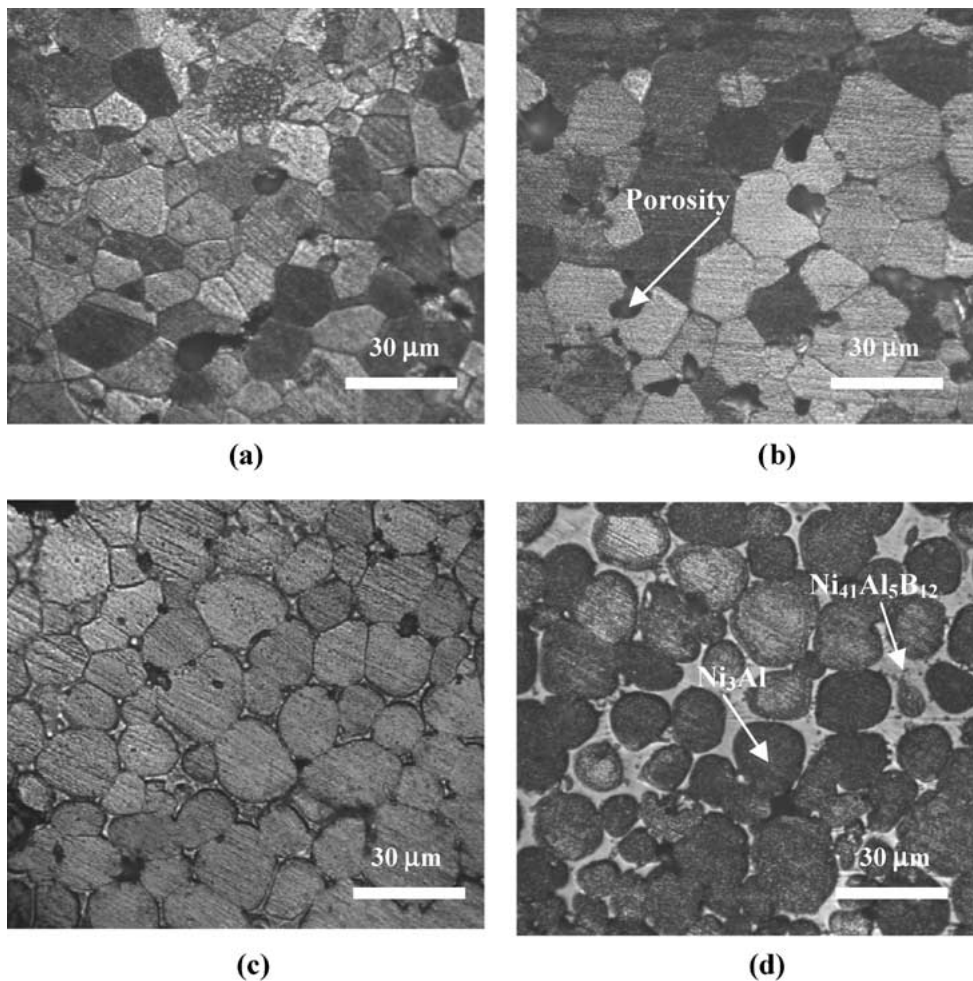


Figure 1 Effect of boron addition on the as-etched microstructure of reaction synthesized nickel aluminides; (a) boron-free ($14\ \mu\text{m}$ average grain size), (b) 0.3 wt% B ($20\ \mu\text{m}$ average grain size), (c) dual-phase region in 0.50 wt% B, and (d) 1.0 wt% Boron.

also impose capillary pressure on the particles. The Al, B and Ni powders were consumed in the reaction synthesis process to produce Ni_3Al and $\text{Ni}_3\text{Al}/\text{Ni}_{41}\text{Al}_5\text{B}_{12}$ microstructures depending on the initial elemental powder composition. The reaction is exothermic and therefore considerable amount of heat is given off. This heat raises the temperature of the product to a maximum temperature. The fact that the compact did not completely melt and kept its cylindrical shape indicates that although the maximum temperature achieved in the reaction was higher than the melting point of the boride

product phases, it did not exceed the melting point of the Ni_3Al major phase present.

SEM/WDS was also used to examine qualitatively the distribution of boron in boron-doped $\text{Ni}_{76}\text{Al}_{24}$ alloy containing 1 wt% boron. The data shown in Fig. 2 indicates that the amount of boron in the matrix is higher than in the Ni_3Al particle, which reconfirm the previous finding.

The formation of this boride phase when the boron content exceeds its solubility limit in Ni_3Al has been reported elsewhere [4, 16]. The crystal structure of the

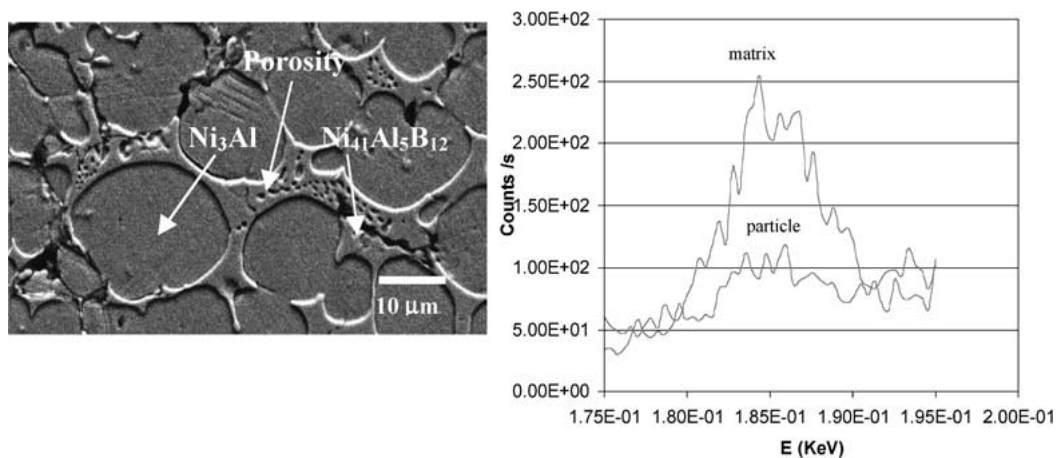


Figure 2 Back scattered image of as etched 1 wt% boron-doped $\text{Ni}_{76}\text{Al}_{24}$ (left); and its WDS measurement for the boron distribution in both Ni_3Al (particle) and $\text{Ni}_{41}\text{Al}_5\text{B}_{12}$ (matrix) (right).

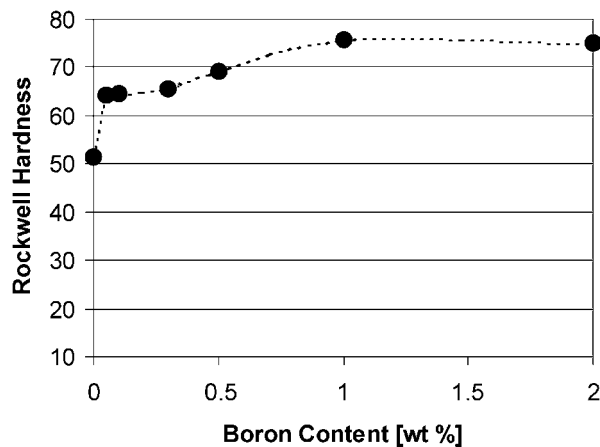


Figure 3 Rockwell hardness of as-prepared nickel aluminides boron-doped alloys (scale A).

phase is identified with an $M_{23}C_6$ -type phase (f.c.c., $a = 10.5 \text{ \AA}$). Using the crystal lattice parameters [17], the theoretical density of $Ni_{41}Al_5B_{12}$ solid structure was found to be $6.85 \text{ g} \cdot \text{cm}^{-3}$.

Fig. 3 shows the effect of boron content on the Rockwell hardness (scale A) of as-prepared boron-doped $Ni_{76}Al_{24}$ alloys. The bulk Rockwell hardness of boron-free Ni_3Al was found to be 51.5 HRA, in good agreement with the value of 52 HRA reported for reaction synthesised Ni_3Al [18]. The figure shows that a small addition of boron increases the hardness of the nickel aluminides showing a slight increase in hardness for boron contents in the range 0.1–0.30 wt%. At 0.50 wt% B-content an additional increase in the hardness was observed, which further increased with boron content up to 2 wt% amounting to an increase up to 50% in hardness compared to the Ni_3Al boron-free. The first increase in hardness could be explained as a solution hardening effect of boron within the Ni_3Al grains, which has also been previously reported [5]. Even though it is well known that boron tends to segregate to Ni_3Al grain boundaries, small amounts of boron can still be present within the Ni_3Al grains as confirmed by SEM/WDS. The second apparent increase in hardness was first observed at 0.5 wt% B, which represents a transition composition from a one-phase to a two-phase microstructure with small amounts of boride

phase formed. At 0.5 wt% B, the microstructure contained regions of equiaxed Ni_3Al single-phase grains and much fewer regions of dual phase microstructure as observed in Fig. 1c. The variation in the observed microstructure may have been due to uneven mixing of the elemental powders leading to slightly uneven distribution of boron at the two phase-region, and therefore, boron may have been in excess of the value at the single-phase regions. Nevertheless a clear transition both in microstructure and hardness is evident. This increase in hardness at and above 0.5 wt% B could be explained in terms of a combined effect of the solution hardening and the formation of the harder boride phase. The same hardness profile observed in Fig. 3 was also obtained using repeat experiments on scale C (150 kg major load using diamond indenter). The hardness data shown in Fig. 3 is the average hardness value of 10 hardness measurements carried out on each specimen. The increased hardness may indicate a possible advantage in the wear properties of the composite compared with the single-phase materials.

Fig. 4 shows the as-etched microstructure of the exuded beads formed during reactive sintering of Boron-doped $Ni_{76}Al_{24}$ containing 2.0 wt% B. The microstructure is two-phase similar to the bulk of the specimen. SEM/EDS revealed the two-phase microstructure as consisting of Ni_3Al (Al-rich particles) + $Ni_{41}Al_5B_{12}$ (matrix) and this was confirmed by XRD and Neutron diffraction measurement. The Rockwell hardness of the beads was also very close to that of the bulk specimen. Although having a dendrite-like appearance, the microstructure is actually similar to that of the bulk specimen, having been squeezed out at weak spots on the cylindrical compact, at highly dense areas where temperatures are also expected to be higher during the reaction. In the beads microstructure, Ni_3Al particles were found to join together in some region and coalesce to form larger particles. The formation of the beads could be explained in terms of the density difference between the two phases that formed during reactive sintering. The calculated theoretical density of solid $Ni_{41}Al_5B_{12}$ is $6.85 \text{ g} \cdot \text{cm}^{-3}$ compared with the density of Ni_3Al , which is equal to $7.5 \text{ g} \cdot \text{cm}^{-3}$. Indeed the formation of an even lower density liquid boride as a result of the combustion energy during the reaction

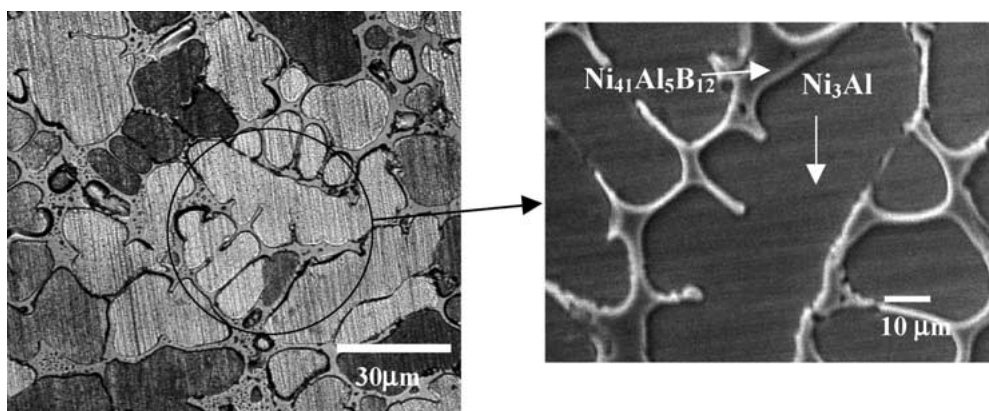


Figure 4 Optical micrograph of the as-etched beads obtained from sample containing 2.0 wt% boron during reactive sintering (left), and its secondary electron image (right).

TABLE I Effect of boron additions on the bulk volume, bulk density and percentage total porosity of as-prepared nickel aluminides using Archimedes principle

Boron content (wt%) ^a	Bulk volume (cm ³)	Bulk density (g/cm ³)	% Total porosity (±1.5)
Elemental pellet	1.34	4.87	30.0
Zero	0.94	6.48	13.5
0.10	0.93	6.87	8.6
0.30	0.94	6.24	13.6
1.00	0.99	6.11	16.5 ^b
2.00	0.99	5.96	16.0 ^b

^aElemental powders stoichiometry of Ni and Al equals 3 : 1 (nickel rich, 76% Ni).

^bCalculated using image analysis results (±2.0%).

will tend to occupy a greater volume than the Ni₃Al. This in addition to the capillary pressure leads to the extrusion or squeezing out of the excess liquid/particle on the compact surface. During this process the liquid boride will carry along with it some of the Ni₃Al particles that have already been formed, resulting in the aggregate-like structure as mentioned.

3.2. Effect of boron addition on the bulk density and total porosity of as-prepared Ni₇₆Al₂₄ alloy

Table I shows the effect of boron addition on the bulk volume, bulk density and percentage total porosity of as-reactively sintered nickel aluminides (boron-doped). The data reveals that the addition of a small amount of boron (0.10 wt%) results in a decrease in the bulk volume and total porosity due to shrinkage. Similar findings have been reported by Munir *et al.* [7], and German *et al.* [6] but to date no clear mechanism has been proposed to explain why the boron addition at this level reduces the total porosity.

Image analysis was used to measure the percentage Ni₃Al/Ni₄₁Al₅B₁₂ phases formed in the bulk specimens. The percentage was found to be equivalent to (80/20 ± 5.5 wt%) and (72/28 ± 4.5 wt%) for the boron content 1.0 and 2.0 wt% respectively with a reduction of the particle size of as-etched Ni₇₆Al₂₄ - 2.0 wt% (9.0 ± 1.1 μm) compared with 1.0 wt% B (14.0 ± 2.0 μm).

The data in Table I, indicates that the B-doped Ni₇₆Al₂₄ alloy containing 1.0 wt% B has a higher bulk density than the 2.0 wt% B. This could be due to the increase in the percentage of the low density Ni₄₁Al₅B₁₂ (6.85 g · cm⁻³) compared to Ni₃Al (7.5 g · cm⁻³).

The data shown in Table I, and the data obtained from SEM/EDS, as previously mentioned, indicates that the formation of boride phase Ni₄₁Al₅B₁₂ (6.85 g · cm⁻³) which contains 5.0 wt% Al lowers the bulk density, and shifts the equilibrium reaction from the Ni₃Al (Ni-rich 76 at.%) to Ni₃Al (Al-rich 26 at.%) compared with boron-free Ni₃Al.

4. Conclusions

A preliminary study of the effect of boron addition on the reactive sintering of Ni₇₆Al₂₄ was carried out. Four main conclusions can be drawn:

1. Two-phase mixtures of Ni₃Al and Ni₄₁Al₅B₁₂ boride phase appear with over 0.5 wt% B additions. The extrusion of beads at the surface for 1.0 wt% B-content and above, is a direct result of the decreased density of the liquid boride formed.

2. All of the boron had either diffused into Ni₃Al or combined with Ni and Al to form Ni₄₁Al₅B₁₂ and no elemental boron was found.

3. The hardness increases with an increase in boron content, due to solution hardening below the solid solubility limit and a combination of solution hardening and harder boride phase formation above the solubility limit of boron in Ni₃Al.

4. The extruding effect of semi-molten beads may be a limiting factor at high B-contents to the application of reaction synthesis for the production of Ni₃Al intermetallic/boride composites.

Acknowledgements

The authors are grateful to the University of Missouri Research board for funding this work, under grant number (RB00-041). Special thanks go to Professors Aaron D. Krawitz and Robert A. Winholtz, Mr. Eric Runde, Dr. J. Yang and Mr. L. Ross for their appreciated help with the Neutron, X-ray diffraction and SEM work.

References

1. V. K. SIKKA, J. T. MAVITY and K. ANDERSON, *Mater. Sci. and Eng.* **A153** (1992) 712.
2. M. PEILI, Y. YING, H. LINGUANG, L. YULIANG and Z. ZENGYONG, *ibid.* **A153** (1992) 377.
3. V. K. SIKKA, M. L. SANTELLA and J. E. ORTH, *ibid.* **A239/240** (1997) 564.
4. C. T. LIU, C. L. WHITE and J. A. HORTON, *Acta Metall.* **339** (1985) 213.
5. G. JIANTING, L. HUI, S. CHAO, W. SHUHE, R. DAGANG, X. LIANGYUE and J. JIAN, *Mater. Sci. and Eng.* **A 152** (1992) 120.
6. R. M. GERMAN, A. BOSE, D. ALMAN, J. MURRAY, P. KORINKO, R. ODDONE and N. S. STOLOFF, First World Conference on Powder Metallurgy, July 1990, p. 310.
7. A. PHILPOT and Z. A. MUNIR, *J. Mater. Sci.* **22**(1) (1987) 159.
8. K. MORSI, H. B. MCSHANE and M. MCLEAN, *Mater. Sci. and Eng.* **A290** (2000) 39.
9. *Idem.*, *Metall. and Mater. Trans.* **A 31A** (2000) 1663.
10. K. MORSI, *Mater. Sci. and Eng.* **A299** (2001) 1.
11. B. H. RABIN, R. N. WRIGHT, J. R. KNIBLOE, R. V. RAMAN and S. V. RALE, *ibid.* **A153** (1992) 706.
12. W. D. CALLISTER, JR, "Materials Science and Engineering: An Introduction," 4th ed. (John Wiley and Sons, New York, 1997).
13. S. T. FRANK, U. SODERUALL and C. HERZIG, *Intermetallic* **5** (1997) 221.
14. Annual Book of ASTM Standards, "Metals-Mechanical-Testing; Elevated and Low-Temperature Tests; Metallurgy" (ASTM 1916 Race street, Philadelphia, PA, USA, 1995) Vol. 3.01, p. 236.
15. M. C. CHATURVEDI, S. BAUERJEE and A. K. JENA, *Scripta Materialia* **36** (1997) 269.
16. J. H. LEE, B. H. CHOE and H. M. KIM, *Mater. Sci. and Eng.* **A 152** (1992) 253.
17. P. VILLARS and L. D. CALVERT, "Pearson's Handbook of Crystallographic Data for Intermetallic Phases" (1985) Vol. 2, p. 1008.
18. W. MISIOLEK and R. G. GERMAN, *Mater. Sci. and Eng.* **A144** (1991) 5.

Received 18 April
and accepted 21 November 2001